Alexandria Engineering Journal (2022) 61, 2775–2786

HOSTED BY

ELSEVIER

Alexandria University

Alexandria Engineering Journal

www.elsevier.com/locate/aej
www.sciencedirect.com

Integrated design of solar photovoltaic power generation technology and building construction based on the Internet of Things

XiuFeng Wu [a,*], ChunYing Yang [b], WeiCHi Han [a,c], ZongRui Pan [d]

[a] *School of Civil Engineering, LiaoNing Technical University, FuXin City, LiaoNing Province, China*
[b] *School of Innovation and Practice, LiaoNing Technical University, FuXin City, LiaoNing Province, China*
[c] *Jangho Group Co., LTD, BeiJing City, China*
[d] *Shenyang Huazhou Heavy Industry Steel Structure Co. LTD, Shenyang City, LiaoNing Province, China*

Received 22 March 2021; revised 23 April 2021; accepted 1 August 2021
Available online 13 August 2021

KEYWORDS

Internet of Things;
Solar energy;
Photovoltaic power generation;
Building construction

Abstract At the same time of economic development, the increasing scarcity of energy has had a great impact on people's development. People's production and life demand for electricity is also increasing rapidly, and solar power technology has received more and more attention. As a new energy source, solar energy has the advantages of environmental protection and sustainability, and it has no regional restrictions, can be used on-site, and designed to scale. Solar power generation is an important way to use solar energy. As the main component of the grid-connected power generation system, solar grid-connected inverters complete the tracking problem of the maximum power point in the photovoltaic array and transmit electrical energy to the grid through a set of control algorithms. The electrical energy is transmitted to the grid through the inverter, consistent with solar energy. In order to solve the problems of low integration, low energy efficiency, low reliability, high power consumption and lack of effective monitoring measures for solar energy devices. This article starts with the design of the solar cell integrated system, and through detailed analysis of the solar production system and building integrated planning, establishes the shadow radiant energy model of the solar cell system building electrical and solar cell system based on the Internet of Things, and designs an object-based Networked comprehensive auxiliary platform. The use of the Internet of Things and ZigBee wireless sensor network to study distributed solar energy devices and realize the joint design of solar energy devices and buildings is of great significance to the development of photovoltaic construction industry.

* Corresponding author.
E-mail address: wuxiufeng@lntu.edu.cn (X. Wu).

Peer review under responsibility of Faculty of Engineering, Alexandria University.

https://doi.org/10.1016/j.aej.2021.08.003
1110-0168

1. Introduction

Today's society is an information society centered on the Internet. Digitization, informationization and world economics are the hallmarks of the current era. With the continuous rapid development of information technology, the process of world economics has been continuously strengthened. The use of computer technology, communication data and the Internet to complete e-logistics and Internet commerce has been widely used in society. The continuous improvement of information technology and information storage is just the prelude to the transformation of the IT industry. The cost of information dissemination is getting less and less, and it is bound to usher in the era of the Internet of Things dominating. As a post-IP product, the Internet of Things is developing rapidly and will become popular in the future. This is a major plan to realize the intelligentization of the world.

The rapid development of the economy and the huge use of energy, the increasing scarcity of energy have a great impact on people's development. Energy is a key element for people's existence and sustainable development, and is the basic guarantee for social and economic development. The number of people in the world is increasing, and the demand for energy continues to rise. Non-renewable energy sources such as petrochemicals are important resources for the current world economic development. The gap between energy supply and energy demand is getting bigger and bigger, so energy prices are also rising, which has seriously affected the rapid development of the world economy. Therefore, sustainable development is the only way for human survival and development. In this century, new energy and renewable energy are playing more and more roles. Because of this, energy-saving and environmentally friendly resources based on the development of new energy and renewable energy has been valued by more and more countries in the world. As the optimization of future high-tech energy production technology, battery devices are composed of clean energy and renewable energy, and are increasingly favored by people.

At the same time of economic development, people's production and life demand for electricity is also increasing rapidly, and solar power generation technology has received more and more attention. As the main component of the grid-connected power generation system, the solar grid-connected inverter completes the tracking problem of the maximum power point in the photovoltaic array, and transmits electric energy to the grid through a set of control algorithms, so that the electric energy is transmitted to the grid through the inverter, consistent with solar energy. The greatest effect of array emission is balance. However, the inverter produced by the inverter still has some problems in quality. For example, the quality of inverters is not stable; because there is no supervision in many places, the safety of solar equipment, including solar panels, has become a major issue. These shortcomings have brought a lot of management and control to the practical application of networked inverters. Therefore, integrating the reverse current into the network requires a lot of work. The most important thing is to monitor the power quality of the inverter. The introduction of the Internet of Things makes solar power generation an efficient and convenient solution, solves the real-time monitoring of power quality and other safety issues, and also maximizes the effectiveness of supporting management decisions. At this time, appropriate computer-assisted support helps to integrate and integrate the building system and photovoltaic installations to achieve a complete integrated design. Therefore, this paper proposes a low-cost, high-efficiency distributed solar cell system based on the Internet of Things technology, which is used for automatic tracking and monitoring of solar cell groups, and realizes the integrated design and building production of solar systems.

2. Related work

The Internet of Things was born in the late 20th century. At the beginning, it refers to obtaining information about the subject through the electronic roof, and then establishing a network where all subjects can communicate with each other through the Internet to obtain intelligent identification, supervision and management of objects. Document [1], Document [2] explained the concept of the Internet of Things is that everything in the world can actively exchange information through the Internet that is, collecting and transmitting information through different entities such as sensor applications, radio frequency identification applications, global positioning applications, infrared sensors, and wireless network applications. With the advancement of technology, real-time collection and transmission of monitored objects or processes are connected and interacted with the Internet to form a huge network. The document [3] records that the Internet of Things as a network is hierarchical, including sensors and sensor networks that collect information, and is responsible for processing and transmitting sensory information through the Internet and mobile communications. The business and application networks are responsible for sensor networks and The transmission network obtains, analyzes and processes relevant information, and makes appropriate management and decisions to realize intelligent management, use and service. Literature [4] shows that the ZigBee Alliance currently has a great influence on the use of the Internet of Things. ZigBee wireless sensor network technology provides great comfort and development space for the application of the Internet of Things in industrial monitoring, smart home, medical and other fields. Literature [5] from the perspective of the development and application of the Internet of Things, the use of distributed solar systems on the Internet is the future development direction of distributed solar systems. Realize the intelligent collection, transmission and monitoring of distributed solar building operating parameters.

Document [6] records that the concept of renewable energy means that energy can be regenerated regularly and cyclically within a certain time span, which is different from the complete disappearance of oil and other energy sources with the disappearance of use. Solar energy, biomass, wind, hydropower and ocean energy are all renewable energy sources. This article focuses on solar energy. The document [7] records that the current solar energy utilization refers to the use of certain procedures to directly collect, convert or store solar energy so that people can use it when needed. Converting solar energy into the energy form needed by human beings efficiently, safely, comfortably and economically requires research on its working principle, control process, design diagram, process technology, and experimental science. Document [8] records the experience of German solar system and analyzes the relationship between the geographical arrangement of solar energy in the solar energy application market and the regional solar system. Literature [9] simulated and analyzed the factors affecting photovoltaic power generation devices, modeled additional photovoltaic power generation devices, and implemented electrical guidance technology. Document [10] records the relationship between solar radiation changes and solar installations, and describes the temporal and spatial distribution of solar output through indicators such as “clear sky factor”, “occlusion index” and “spatial coefficient”, and establishes the mathematics of solar installations in specific areas model. Literature [11] contacted the PVsyst software to design and select the photovoltaic solar cell device of the urban roof building. By selecting the load, the cascade inverter scheme was designed, and finally the applicability of the design form was verified. From the perspective of electrical control, the real-time maximum output of the BIPV project is achieved. The document [12] records that the photovoltaic module grid-connected inverter is controlled, the MPPT control logic is analyzed in detail, and the interference support climbing method is planned according to the characteristics of the photovoltaic module. MPPT control strategies such as components and adopting incremental methods have increased the power generation efficiency of new energy.

Construction, industry and transportation are the three major energy consumption industries. Document [13] records that the amount of construction loss can directly reflect the development of the tertiary industry and the country’s development speed. The more building energy consumption, the better the daily life of people, and it also reflects the economic development to a certain extent. In the technology of distributed solar power plants, scholars are constantly exploring the integration of solar modules into building materials or structures, and efficient integration of new energy power generation technologies with urban buildings. This technology is already photovoltaic building integration. Document [14] and Document [15] record that photovoltaic installation not only overcomes the problems of large-scale centralized photovoltaic power station occupancy and maintenance, but also has the advantages of local power generation loss, reduction of civil construction and installation costs, and power saving. This is a new goal pointed out by the current development of solar energy technology in my country. Regarding the benefits of government building integration, the document [16] records that Internet solar cell devices are generally placed on the roof or outer wall of a building, and there is no extra space or equipment. Suitable for use in densely populated places. It is used in buildings and office areas, especially in cities where every inch of land is expensive. Due to the modularization of solar panels, the installation of solar panels is more convenient, and the installed capacity can be selected according to the power consumption of the load. The document [17] records that because the solar energy system is installed on the roof or exterior wall of the building to convert solar energy into electricity, the outdoor temperature is lowered, and the cooling load of the air conditioner will also be reduced, which not only saves resources It also ensures good indoor air and avoids environmental pollution caused by the use of traditional fuels for power generation [18].

3. Application research of Internet of Things in solar photovoltaic power station monitoring and management system

3.1. Overall design scheme of optical tracking transmitter

The overall design of the optical tracker is shown in Fig. 1. The light intensity transmitter is mainly based on the light intensity signals collected by the four photosensitive sensors and the automatic group control tracking software algorithm to realize the detection and control of the light intensity [19]. The light tracker rotating platform mainly completes the capture and detection of light intensity signals and the light tracker tracks and changes with the changes of the sun; the control card mainly realizes the group’s automatic tracking control algorithm, engine control and automatic tracking group signal transmission.

Fig. 2 shows the specific situation of the mechanical structure.

In Fig. 2A–C are the photosensitive sensor board, the vertical axis stepper motor accessory and the horizontal axis stepper motor console. The horizontal axis stepping motor M can realize the rotation of the orientation detection from 0 to 180,

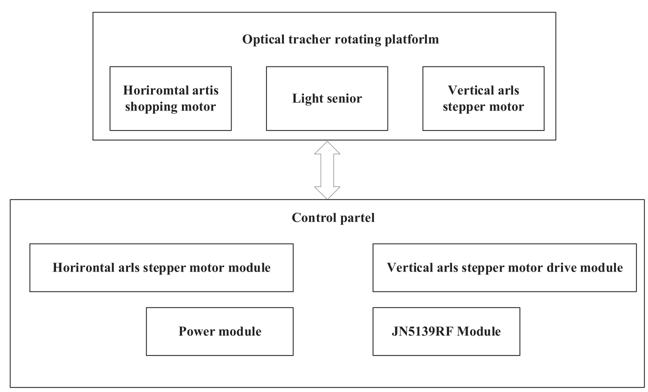

Fig. 1 Block diagram of overall design of optical tracking transmitter.

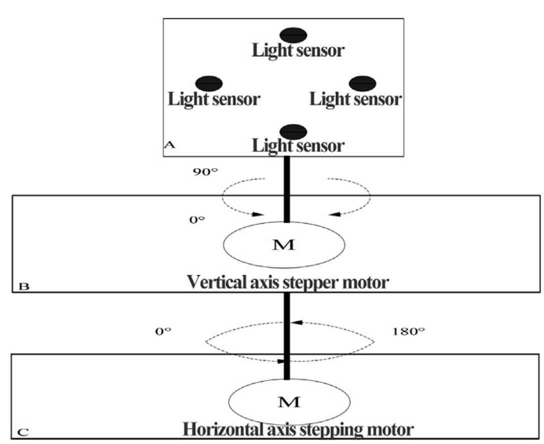

Fig. 2 Mechanical structure of optical tracking transmitter.

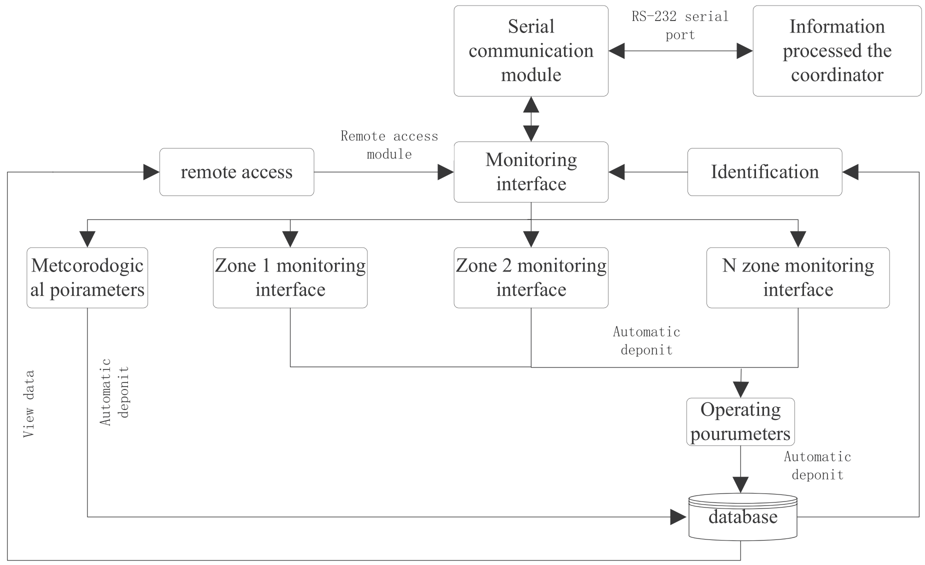

Fig. 3 Monitoring and management software design scheme.

Table 1 API functions.

Function name	Function of function
createFil	Create file
closeHandl	Stop file
getCommStat	Read port parameters
setCommStat	Set serial port parameters
readFil	Get port data
clarCommError	Remove port errors
purgComm	Remove port buffer

and the vertical axis stepping motor can realize the rotation of the vertical axis from 0 to 90. The tracking mechanical unit of the optical tracking transmitter should adopt dual-axis tracking control to realize the tracking and detection of the height and azimuth positioning of the two-dimensional and three-dimensional sunlight [20].

3.2. Software and hardware design of photovoltaic power station monitoring and management system

3.2.1. System software design of photovoltaic power station

The design of photovoltaic control software and application control monitoring system is based on the network and application layer of the Internet of Things technology. The system software can retrieve the operating data of the photovoltaic power station in real time from the recording layer, and prompt, record and remind the abnormal data [21]. These data can provide fast, efficient and personalized services for maintenance, operation and demand personnel, reduce the cost of distributed photovoltaic installation, improve the stability of distributed photovoltaic installation, realize remote access and demand monitoring, and Internet-based distributed buildings Operation of parameter port information in the central database of the photovoltaic installation management system. The details are shown in Fig. 3.

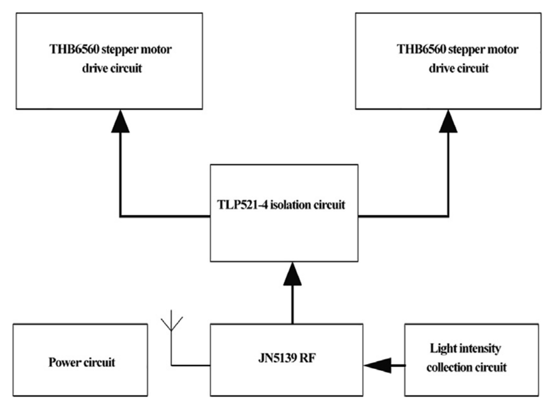

Fig. 4 Optical tracking transmitter hardware structure block diagram.

The development system used in this design is C++Builder, through which the software is completed using WindowsAPI features. This design is constructed with C++: The tool functions and function functions in the serial communication group API are shown in Table 1.

3.2.2. Optical tracking transmitter hardware design

Fig. 4 is a detailed architecture diagram of the optical tracking transmitter.

3.3. Common fault detection methods of photovoltaic self-tracking power generation system

3.3.1. Analysis of common system failures

As there are more facilities in the photovoltaic grid-connected power generation system, there are more problems in the system. The commonly used fault types and detection methods are shown in Table 2.

Table 2 Common fault types and detection methods.

Fault type	Visual inspection	Multimeter measurement	I/V curve measurement	Inverter reading	AC line inspection
Dirty surface of photovoltaic element	√		√		
Short circuit of photovoltaic element			√	√	
Diode short circuit		√		√	
Photovoltaic component hot spot		√	√	√	√
Delamination of glass and back film	√		√	√	
The photovoltaic element junction box dropped		√		√	
Photovoltaic component wire aging	√	√	√	√	√
Photovoltaic cell line break		√	√		√
Yellow battery	√	√	√		
Diode blocking			√	√	
Inverter harmonics are not matched					√
Linear voltage interference					√
Low inverter efficiency				√	√
Destroyed fuse		√			
Voltage protector destroyed		√			
Track mechanical damage	√				
Stepper motor destroyed		√			

Table 3 Analysis table of photovoltaic array status.

Fault type	Array output voltage	Array output current	Module output voltage	Module output current	Abnormal working battery component temperature
Photovoltaic destruction	No change	Cut back	Cut back	Cut back	Variety
PV temperature rise	No change	Reduce	Cut back	Constant	Variety
Photovoltaic shelter	No change	Cut back	Cut back	Cut back	Variety
Main line disconnected	No change	No	Cut back	Module output current	Abnormal working battery component temperature

3.3.2. State analysis of solar photovoltaic array

Table 3 is the status of the photovoltaic array.

3.3.3. Design of online estimation method for photovoltaic module parameters

Generally, the scale of performance test is relatively large, and solar cell installations are generally in open areas, making it difficult to conduct on-site inspections. Therefore, using the estimation method of battery module performance parameters, the online detection of battery module performance is completed. This method can only record the light intensity received by the battery pack and the temperature of the battery pack to estimate the maximum voltage Um, maximum current Im, and open-circuit voltage Uoc of the battery. The short-circuit current Isc on the capture card is used to complete the battery acquisition performance.

The current equation of the solar module is:

$$I = I_{ph} - I_O\left\{\exp\left[\frac{q(U + IR_s)}{AkT}\right] - 1\right\} - \frac{U + IR_s}{R_{sh}} \tag{1}$$

The component is short-circuited, U = 0, the diode does not light up, and the current flowing through the OI is very small and can be ignored. The above formula (1) can be modified as follows:

$$I_{sc} = \frac{I_{ph}}{1 + \frac{R_s}{R_{sh}}} \tag{2}$$

When the component is opened, there am I = 0, formula (1) can be changed to:

$$I_{ph} = I_O\left[\exp\left(\frac{qU_{OC}}{AkT}\right) - 1\right] + \frac{U_{OC}}{R_{sh}} \tag{3}$$

When the solar module is running at the maximum power point, formula (1) can be changed to:

$$I_m = I_{ph} - I_O\left\{\exp\left[\frac{q(U_m + I_m R_s)}{AkT}\right] - 1\right\} - \frac{U_m + I_m R_s}{R_{sh}} \tag{4}$$

By deriving the current Eq. (1) of the component at the maximum power point of the component Pm, we can get:

$$\frac{U_m}{I_m} = R_s + \frac{AU_T R_{sh}}{AU_T + (R_{sh} + R_s)(I_{sc} - I_m) - U_m} \tag{5}$$

In the formula, UT is the thermal voltage, and the formula is:

$$U_T = \frac{kT}{q} \tag{6}$$

The diode reverse saturation current I0 can be expressed as:

$$I_o = I_{o-STC}\left(\frac{T}{T_{STC}}\right)^3 e^{\frac{E_G}{A}\left(\frac{1}{U_T} - \frac{1}{U_{T-STC}}\right)} \tag{7}$$

Under standard conditions, absolute temperature can be expressed as:

$$I_{o-STC} = \frac{I_{sc-STC}}{\exp\left(\frac{U_{oc-STC}q}{AkT}\right)} \tag{8}$$

The formula for calculating optical flow is:

$$I_{ph} = \frac{S}{S_{STC}}[1 + u_i(T - T_{STC})]I_{O-STC} \tag{9}$$

The estimation method of RS and RSh is:

$$R_s = \frac{U'_m - U_m}{I_m} \tag{10}$$

$$R_{sh} = \frac{U'_m}{I'_m - I_m - I_o\left[\exp\left(\frac{qU'_m}{AkT}\right) - \exp\left(\frac{qU_m}{AkT}\right)\right]} \tag{11}$$

By measuring ISC and UOC under different illumination. The ideal factor A of the diode is:

$$A = \frac{U_{ocl} - U_{oc2}}{\frac{kT}{q}\ln\left(\frac{I_{sc1}}{I_{sc2}}\right)} \tag{12}$$

The new photovoltaic array detection method will only find the general orientation of the problematic battery module according to the voltage and current changes of each measurement node when the solar energy fails. Once the location of the defective battery component is found, the battery components in the area must be checked online one by one, and the defective battery component will be found. The error detection method of the new photovoltaic array is shown in Fig. 5.

3.4. System operation simulation experiment test and analysis

3.4.1. Solar energy utilization potential test

Typical weather data is mainly used to simulate building loads. The outdoor meteorological parameters in this article are classical data in the TMY2 format obtained by the weather station. Manage the data of a typical weather year at a specific location, showing the external dry bulb and wet bulb temperatures and the horizontal solar radiation conditions shown in Figs. 6 and 7 (see Fig. 8).

The typical weather year weather data is mostly used in building load simulation. The outdoor weather calculation parameters in this paper adopt the typical weather year data in TMY2 format obtained by Meteonorm(v7.1). The typical meteorological year data is composed of 12 months with typical local climate. Taking the monthly average of meteorological parameters in the past 10 years as a reference, the months close to the reference value of the past 10 years are selected

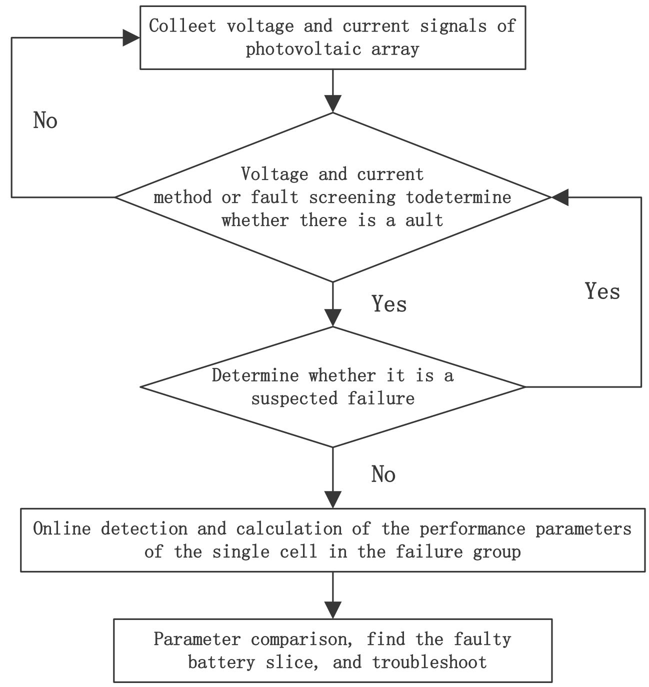

Fig. 5 Solar photovoltaic array fault detection method.

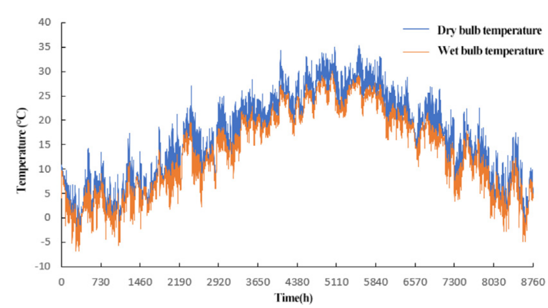

Fig. 6 Outdoor dry and wet bulb temperature in a typical weather year.

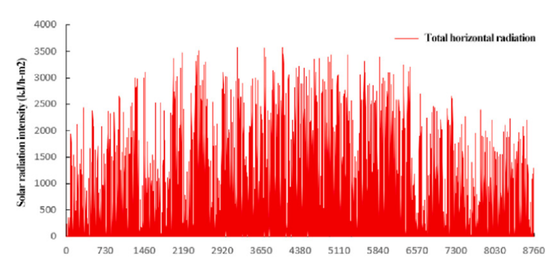

Fig. 7 Solar radiation intensity at horizontal plane in a typical meteorological year.

from the meteorological data of the past 10 years to form a typical weather Year, representing the meteorological laws of the region. By reading the data of a typical meteorological year in a certain place, the outdoor dry and wet bulb temperature and the horizontal solar radiation intensity obtained are shown in Figs. 6 and 7.

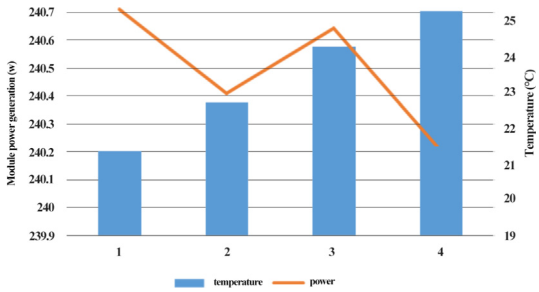

Fig. 8 The relationship between temperature and solar output power.

Table 4 Meteorological parameters during heating period.			
Month	Days	Monthly average temperature (°C)	Monthly average solar radiation (MJ/m^2.d)
12	31	7.5	8.28
1	31	4.8	6.92
2	29	7.1	11.49

It can be seen from Fig. 7 that the level of sunlight in a certain place varies greatly during the day. In general, solar energy is stronger in summer and transitional periods than in winter. The meteorological parameters during the heating period are summarized in Table 4. It can be seen that the average level of exposure during the entire heating period is 792,68 MJ/m^2, which is 220,18 kWh/m^2; the average daily exposure is 8,82 MJ/m^2, and the solar energy potential is huge.

3.4.2. Tracking test results

The first is to download the corresponding programs to the optical tracker, ZigBee terminal assembly point and ZigBee coordinator, integrate the two solar devices on the optical tracking transmitter, automatic tracking device and connection device, and then connect the two sets of devices Set in a different location; perform detection and register power generation voltage parameters at any time, and the power and power generation of the two solar installations should also be registered at any time. Solar installation tracking monitoring power generation parameters are shown in Table 5, and fixed solar panels production parameters are shown in Table 6.

3.5. Data anomaly detection and correction

3.5.1. The influence of temperature on photovoltaic output power

The figure below is the power generation curve of experimental solar modules at different temperatures. It can be seen that temperature is basically inversely proportional to the amount of electricity generated. The higher the temperature, the lower the power and the less electricity that can be generated. Therefore, the influence of atmospheric temperature should be considered in the forecast of solar cells.

3.5.2. The prediction algorithm model of photovoltaic power generation power

Solar energy is actually a gray system. In practice, there are many unstable situations that affect the output performance of solar power plants. In order to judge the power generation, the gray theory can be used to establish a model. The process is:

First give the original order:

$$x^0 = \{x^0(1), x^0(2), ..., x^0(n)\} \tag{13}$$

Perform accumulation to generate a new sequence:

$$x^1 = \{x^1(1), x^1(2), ..., x^1(n)\} \tag{14}$$

The cumulative method of generating a new sequence is as follows:

$$x^1(k) = \sum_{m=1}^{k} x^0(m), k = 1, 2, ..., n \tag{15}$$

Perform operations on the new sequence generated by the above formula, and the derivative is:

$$\frac{dx^1}{dt} + ax^1 = b \tag{16}$$

Table 5 Photovoltaic panels track and monitor power generation parameters.

Time	Voltage (V)	Current (A)	Power generation (w)	Power generation (wh)
7:00	2.6	0.3	0.6	
7:30	3.6	0.8	3.16	0.92
8:00	5.86	1.2	6.45	2.38
8:30	7.8	2.24	17.63	6.03
9:00	8.6	2.32	19.65	9.32
9:30	8.8	2.41	21.37	10.26
10:00	8.99	2.43	21.74	10.78
10:30	8.98	2.47	22.13	10.97
11:00	9.1	2.48	22.42	11.14
11:30	9.09	2.52	22.78	11.32
12:00	9.2	2.54	23.03	1.46
12:30	9.3	2.56	23.47	11.63
13:00	9.26	2.58	23.78	11.9
13:30	9.36	2.64	24.58	12.08

Table 6 Monitoring power generation parameters of fixed photovoltaic panels.

Time	Voltage (V)	Current (A)	Power generation (w)	Power generation (wh)
7:00	2	0.06	0.06	
7:30	1.6	0.2	0.16	0.06
8:00	2.4	0.16	0.346	0.13
8:30	3.4	0.36	1.16	0.38
9:00	4.6	0.7	2.8	0.97
9:30	5.9	1.2	6.39	2.28
10:00	6.8	1.68	11.53	4.49
10:30	7.8	2.21	17.39	7.24
11:00	8.4	2.25	18.58	9.1
11:30	8.6	2.4	19.56	9.55
12:00	8.9	2.39	20.95	10.13
12:30	9.2	2.53	22.94	10.98
13:00	9.3	2.55	23.38	11.59
13:30	9.35	2.7	24.29	11.92

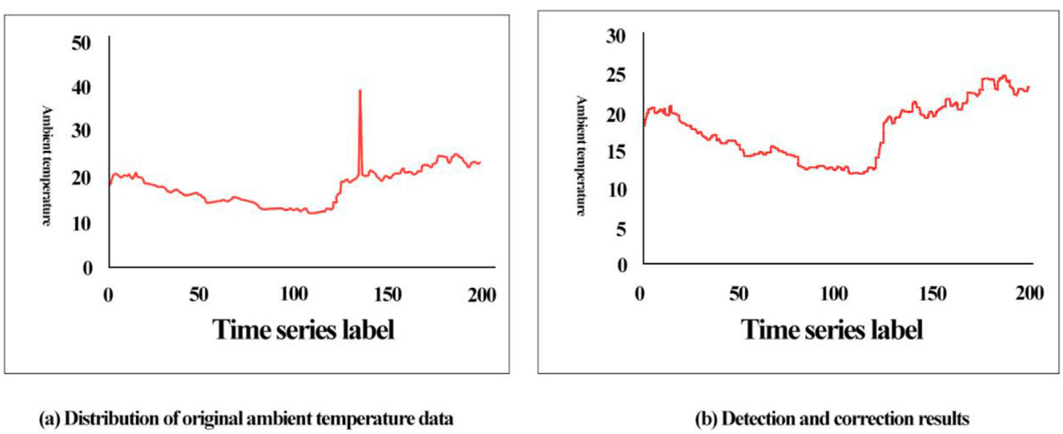

Fig. 9 Ambient temperature data.

In the above formula: a and b are the parameters of the gray model, and the calculation formula for these two parameters is:

$$h = \begin{bmatrix} a \\ b \end{bmatrix} = \left(B^T B\right)^{-1} B^T Y_n \tag{17}$$

$$B = \begin{bmatrix} -\frac{1}{2}(x^1(1) + x^1(2)) & 1 \\ -\frac{1}{2}(x^1(2) + x^1(3)) & 1 \\ \cdots & \cdots \\ -\frac{1}{2}(x^1(n-1) + x^1(n)) & 1 \end{bmatrix} \tag{18}$$

$$Y_n = \left[x^0(2), x^0(3), ..., x^0(n)\right]^T \tag{19}$$

The prediction function obtained by solving the differential equation is:

$$\begin{cases} x^1(k+1) = \left(x^0(1) - \frac{b}{a}\right)e^{-ak} + b/a \\ x^0(k+1) = \hat{x}^1(k+1) - \hat{x}^1(k) \end{cases} \tag{20}$$

3.5.3. Correction of outliers

In order to determine the abnormal value of the actual data of the solar energy device in a period of time, the detection and correction of the ambient temperature are shown in the following figure: Fig. 9(a) is the distribution of the original temperature data, and Fig. 9(b) is the data after the detection and correction. Fig. 9(a) shows the abnormal values in the raw temperature data.

4. Development of integrated computer-aided design system for solar photovoltaic buildings

4.1. Factors affecting the effectiveness of photovoltaic buildings

There are many factors that interfere with the energy saving of photovoltaic installations. In order to accurately determine the energy saving effect of photovoltaic installations, it is necessary to analyze the interference.

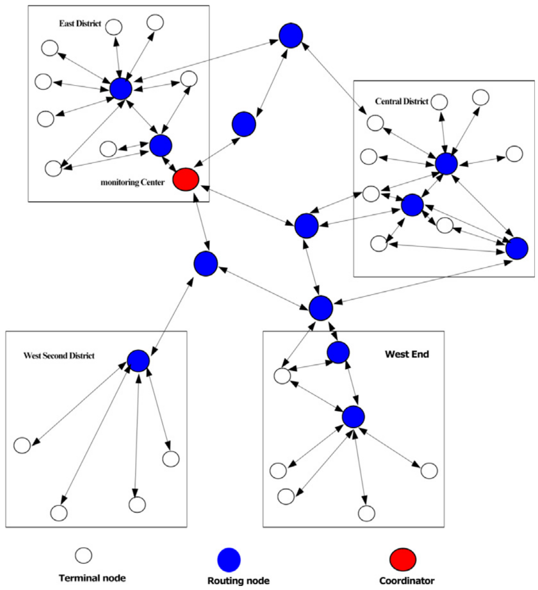

Fig. 10 ZigBee networking and data transmission scheme.

(1) Local meteorological parameters. The longitude and latitude of the project, solar conditions, average temperature, rainfall, air humidity, liquid dust, wind pressure, geographical conditions, etc. will all interfere with solar energy, and also greatly affect the benefits of the project.
(2) Construction. Solar energy is placed on the roof at an angle. Therefore, the orientation, distance and shape of the building will have a certain effect on the solar installation. In order to ensure the nominal impact of the square array, improve the efficiency of photovoltaic installation, reduce the production cost of photovoltaic power plants, and avoid shadows is very important.
(3) PV installed capacity. The photoelectric conversion efficiency of photovoltaic installations, system operating losses, solar module types and inverter types all interfere with the energy-saving effect of photovoltaic installations.

4.2. Evaluation basis for energy-saving efficiency of integrated photovoltaic systems

4.2.1. ZigBee networking and data transmission scheme

In this paper, ZigBee self-organizing wireless sensor network is used to transmit the operating parameter data of the building photovoltaic power station to the coordination node in a multi-hop manner, and then the coordinator connects with the PC through the RS232 serial port to display the operating parameters of the building solar system. Monitor and manage the construction of solar installations and remote access solutions. The ZigBee network and data transmission schedule is shown in Fig. 10:

4.2.2. Lighting resource conditions

Table 7 shows the statistics of solar radiation in construction area.

4.2.3. Available building area

Table 8 shows the area of profitable use of solar energy installed on the roof of the workshop.

4.3. Efficiency analysis of integrated photovoltaic buildings

4.3.1. Inclined surface calculation model

When installing solar modules at 0 degrees outside the red-brown line, a corresponding degree of inclination must be provided to the 0 degree direction to cover high places to receive relatively more solar energy. In order to determine the amount of solar radiation on a slope facing the equator, the commonly used calculation method is:

$$Ht = Hbt + Hdt + Hrt \tag{21}$$

Calculation formula is: as the season changes, the sun will also change. According to the Kucho equation, calculate the equatorial angle of the sun, the formula is:

$$\delta = 23.45\sin(360 * (284 + n)/365) \tag{22}$$

Table 7 Solar radiation statistics.

Month	Total radiation (MJ/m^2)	Total radiation (kWh/m^2)	Total daily radiation (kWh/m^2)	Average daily direct radiation (kWh/m^2)	Average daily scattered radiation (kWh/m^2)
1	224.2	62.251	2.009	1.178	0.832
2	324.3	90.057	3.217	1.892	1.326
3	466.8	129.695	4.185	2.378	1.806
4	547.88	152.187	5.074	2.444	2.64
5	635.3	176.445	5.693	3.365	2.329
6	583.5	162.057	5.403	3.113	2.28
7	539	149.445	4.822	2.318	2.504
8	505.3	140.334	4.528	2.218	2.311
9	453.59	125.995	4.201	2.288	1.913
10	357	98.888	3.191	1.805	1.387
11	258.5	71.779	2.394	1.425	0.969
12	210.4	58.418	1.885	1.107	0.778
Year	5103.16	1417.543	46.588	25.523	21.068

Table 8 Statistics of available area at the top of the workshop.

Numbering	Name of structure	Roof area /m^2	Usable area /m^2
1	Workshop A	7120.9	4537
2	Workshop B	7120.9	4537
3	workshop C	7120.9	4537
4	workshop D	7120.9	4537
Subtotal		28483.6	18,148

Table 9 Comparison of various slopes.

Inclination	Summer radiation (wh/m^2)	Annual radiation (wh/m^2)	Monthly mean square deviation
30	594,417	1996084.2	37,925
32	587,299	2000948.3	35,987
34	579,465	2003374.8	34,049
36	570,948	2003382.4	32,127
38	561,975	2001213.8	30,255
40	552,336	1996792.9	28,435
42	542,448	1990384.7	26,659
44	531,919	1981757.6	24,963
46	521,004	1970991.2	23,374
48	509,471	1957841.3	21,895
50	497,318	1942305.9	20,556

The calculation of the angle at sunset depends on the specific circumstances:

$$hs = \cos^{-1}(-\tan\phi\tan\delta) \tag{23}$$

$$hs' = \min\{hs, \cos^{-1}(-\tan(\phi - s)\tan\delta)\} \tag{24}$$

The formula used to calculate the direct radiation on a plane in technical applications is:

$$Rb = \frac{H_{bt}}{H_b} \tag{25}$$

Calculating the amount of scattered radiation in the sky on a slope usually includes two parts, one is the box-shaped radiation of the sun beam, and the other is the scattered radiation evenly distributed in the sky, specifically:

$$Hdt = H_d\left[\frac{H_b}{H_0}Rb + 0.5\left(1 - \frac{H_b}{H_0}\right)(1 + \cos s)\right] \tag{26}$$

When the plane faces the equator, the total radiation H, the direct radiation of the sun and the scattered radiation of the sky, H is the reflected radiation of the earth itself, specifically:

$$H_{rt} = 0.5\rho H(1 - \cos s) \tag{27}$$

Based on the above recognition of a specific location, the independent variable S is the inclination of the site, and other radiation doses are its dependent variables. Specifically is:

$$H_t = H_{bt}(s) + H_{dt}(s) + H_{rt}(s) \tag{28}$$

4.3.2. Tilt test of rooftop photovoltaic array

The simplest way of solar energy system is to place solar panels on the building. This article focuses on the inclination and azimuth angles of solvent inclusions designed for this platform. Generally speaking, residents consume the most electricity in summer and solar power is also the most. Solar energy can supplement the demand for electricity. Therefore, the purpose of the array is to obtain more solar radiation in summer. See Table 9 for details.

4.4. Assessment of sustainability of photovoltaic buildings

4.4.1. Analysis of emergy input–output of photovoltaic system

The energy conversion rate converts different types of energy that cannot be compared with other methods in the building solar system into comparable, aggregated solar standards, so that the actual values of different types and energy levels can be measured and compared. See Table 10 for details.

4.4.2. Experimental results of different flow rates in a fixed collector area

Table 11 shows the experimental results of solar dual-energy hot water collection under different flow conditions in the solid heat collection area.

4.4.3. Experimental results under different heat collection areas

Table 12 shows the test results of the hot water collection system when the hot water collection area is different and the water volume of the hot water storage tank remains unchanged. It can be seen that when the heat collection area decreases, the thermal efficiency of the system increases. The main reason is that when the water tank has a certain amount of water and the same radiation, even if the heat collection area increases, the increase in heat will increase to a certain extent, but on the one hand, the heat output of the system, on the other hand, the final temperature of the water tank will also be Decrease, leading to a further increase in calories. The increase in heat and the loss of heat also compete with each other, and the increase in heat level dominates, thereby reducing the thermal efficiency of the system.

4.5. Countermeasures and suggestions for the development of integrated photovoltaic building solar applications

The countermeasures and suggestions for the comprehensive application of photovoltaic installations are:

(1) Interactive application of solar power station and passive building energy saving technology

It can be seen from the above research that the solar energy system is an energy-saving system integrating active and passive design. The solar energy system can significantly cool the room in summer, but under the heat transfer performance of the solar energy envelope, the internal temperature will still exceed the predetermined comfortable temperature range. The reasonable layout of the building direction and the improvement of the thermal insulation technology of the envelope structure can enhance the indoor comfort and reduce energy consumption.

Table 10 Energy value analysis table of building photovoltaic system.

Classification	Project	Raw data	Emergy conversion rate/ (SeJ/unit)	Solar energy value//sej
Renewable resource emergy	Solar radiant energy	4.79×10^{18}J/a	2Sej/J	4.79 × 10″sej
Non-renewable resource emergy	Battery raw materials	6.3×10^{6}/yuan	3.47×10^{12}sej/yuan	2.16 × 10′8sej
	Auxiliary equipment	3.1×10^{5} yuan	3.47×10^{12}sej/yuan	1.05 × 10′8sej
Input emergy	service	9×10^{4} yuan	3.47×10^{12}sej/yuan	2.78 × 10″sej
	Operation and maintenance installation	2.5×10^{4} yuan /a	3.47×10^{12}sej/yuan	8.31 × 10′6sej
Reuse emergy	Commodities (glass, steel, copper, aluminum, plastic, etc.)	5.17×10^{7} g	1.5×10^{9}sej/g	7.23 × 10′6sej
Output energy	Electricity	1.05×10^{12}J/a	1.7×10^{5}sej/J	1.67 × 10″sej

Table 11 Experimental results under different flow rates of fixed heat collecting area.

Time	Flow, m^3/h	First temperature, °C	Medium temperature, °C	Get hot, °C	Ambient temperature, °C	Average radiation intensity, W/m^2	Total radiation, MJ/ m^2	Thermal efficiency
2019.04.09	2.3	18.2	50.2	147.9	15.9	544.1	14.8	45.4%
2019.04.11	2.3	18.2	62.6	205.2	18.9	682.4	19.6	47.8%
2019.04.12	2.3	19.7	65.9	213.5	22.7	695.4	19.8	48.8%
2019.04.14	2.3	19.7	66.7	217.2	25.6	693.8	20.1	49.4%
2019.06.12	3.1	22.6	68.8	214.5	25.8	717.7	20.5	47.9%
2019.06.13	3.1	24.6	63.4	179.4	24.2	639.8	18.5	44.3%
2019.06.15	3.1	26.2	71.4	208.9	29.7	704.9	20.2	47.2%
2019.06.16	3.1	26.5	67.4	189.1	32.8	587.2	16.8	50.9%
2019.07.25	4.1	31.5	74.3	197.8	35.6	668.7	18.8	47.7%
2019.07.26	4.1	33.2	74.6	191.4	34.9	674.6	19.5	44.9%
2019.07.28	4.1	30.6	64.8	158.8	35.4	500.7	14.5	50.2%
2019.07.29	4.1	32.8	70.5	173.8	35.8	583.5	16.9	46.8%

Table 12 Experimental results of system hot water collection under different heat collection areas.

Time	Flow, m^3/h	First temperature, °C	Medium Temperature, °C	Get hot, °C	Ambient temperature, °C	Average radiation intensity, W/m^2	Total radiation, MJ/ m^2	Thermal efficiency
2019.04.09	45	47.5	79.3	152.1	12.8	686.7	15.1	23.1%
2019.04.11	45	27.2	68.5	197.5	14.9	715.6	13.3	33.8%
2019.04.12	34	14.7	58.7	203.4	16.8	483.3	13.8	45.2%
2019.04.14	34	14.4	71.6	264.4	15.4	676.2	18.5	43.7%
2019.06.12	34	16.8	70.5	247.3	19.8	606.6	16.9	44.7%
2019.06.13	34	17.5	80.6	291.6	16.1	774.5	21.1	42.2%
2019.06.15	12	31.8	61.6	136.9	37.6	733.6	21.3	58.8%
2019.06.16	12	31.9	57.8	120.7	37.1	729.5	20.8	52.5%

(2) Improve the utilization rate and specification diversity of solar modules

The price of solar energy systems in buildings is relatively high, and the cost of installation is relatively large. Because solar cell raw materials are insufficient and need to be imported to a certain extent, it is necessary to discover new materials and increase the research and development of new materials, so as to reduce the cost of solar cells, improve the efficiency of solar devices, and reduce the adverse impact on the environment.

5. Conclusion

As a new energy source, solar energy has the advantages of environmental protection and sustainability, and it has no regional restrictions, can be used on-site, and designed to scale. Solar power generation is an important way to use solar energy. In order to solve the problems of low integration, low energy efficiency, low reliability, high power consumption, and lack of effective monitoring measures for solar energy devices. This article starts with the design of the solar cell integrated system, and through detailed analysis of the solar production system and building integrated planning, establishes the shadow radiant energy model of the solar cell system building electrical and solar cell system based on the Internet of Things, and designs an object-based Networked comprehensive auxiliary platform. The use of the Internet of Things and ZigBee wireless sensor network to study distributed solar energy devices and realize the joint design of solar energy devices and buildings is of great significance to the development of photovoltaic construction industry.

Declaration of Competing Interest

The authors declare that they have no known competing financial interests or personal relationships that could have appeared to influence the work reported in this paper.

References

[1] Y. Li, T. Lee, Y. Qian, Analysis and modeling of F0 contours for Cantonese text-to-speech, ACM Trans. Asian Lang. Information Process. (TALIP) 3 (3) (2004) 169–180.
[2] K. Bali, P.P. Talukdar, N.S. Krishna, A.G. Ramakrishnan, Tools for the development of a Hindi speech synthesis system, Proc Fifth ISCA Workshop on Speech Synthesis, 2004.
[3] B. Narasimhan, R. Sproat, G. Kiraz, Schwa-deletion in hindi text-to-speech synthesis, Int. J. Speech Technol. 7 (4) (2004) 319–333.
[4] J. Rama, A.G. Ramakrishnan, R. Muralishankar, R. Prathibha, A complete text-to-speech synthesis system in tamil, in: Proc: WSS, 2002, pp. 191–194.
[5] S. Talesara, H.A. Patil, T. Patel, H. Sailor, N.A. Shah, Novel Gaussian filter-based automatic labeling of speech data for tts system in gujarati language, in: Proc: ICALP, 2013, pp 139–142.
[6] S.P. Panda, A.K. Nayak, Integration of fuzzy if-then rule with waveform concatenation technique for text-to-speech synthesis in Odia, in: Proc: 13th IEEE International Conference on Information Technology, 2014, pp. 88–93.
[7] C. Christogiannis, T. Varvarigou, A. Zappa, Y. Vamvakoulas, C. Shih, A. Arvaniti, Construction of the acoustic inventory for a greek text-to-speech concatenative synthesis system, in: Proc: IEEE International Conference on Acoustics, Speech, and Signal Processing, 2002, pp. II929–II932.
[8] R. Maia, M. Akamine, M.J.F. Gales, Complex cepstrum for statistical parametric speech synthesis, Speech Commun. 55 (5) (2013) 606–618.
[9] R. Maia, M. Akamine, On the impact of excitation and spectral parameters for expressive statistical parametric speech synthesis, Comput. Speech Lang. 28 (5) (2014) 1209–1232.
[10] S.P. Panda, A.K. Nayak, An efficient model for text-to-speech synthesis in Indian languages, Int. J. Speech Technol. 18 (3) (2015) 305–315.
[11] S.P. Panda, A.K. Nayak, A waveform concatenation technique for text-to-speech synthesis, Int. J. Speech Technol. 20 (4) (2017) 959–976.
[12] L. Besacier, E. Barnard, A. Karpov, T. Schultz, Automatic speech recognition for under-resourced languages: a survey, Speech Commun. 56 (2014) 85–100.
[13] S.P. Panda, A.K. Nayak, A rule-based concatenative approach to speech synthesis in Indian language text-to-speech systems, in: Proc: Intelligent Computing, Communication and Devices, Springer, 2015, pp. 523–531.
[14] Z. Handley, Is text-to-speech synthesis ready for use in computer-assisted language learning, Speech Commun. 51 (10) (2009) 906–919.
[15] K.F. McCoy, J.L. Arnott, L. Ferres, M. Fried-Oken, B. Roark, Speech and language processing as assistive technologies, Comput. Speech Lang. 27 (6) (2013) 1143–1146.
[16] M. Bates, The use of syntax in a speech understanding system, IEEE Trans. Acoust. Speech Signal Process. 23 (1) (1975) 112–117.
[17] S. Möller, U. Jekosch, J. Mersdorf, V. Kraft, Auditory assessment of synthesized speech in application scenarios: two case studies, Speech Commun. 34 (3) (2001) 229–246.
[18] S.P. Panda, A.K. Nayak, S. Patnaik, Text-to-speech synthesis with an Indian language perspective, Int. J. Grid Util. Comput. 6 (3–4) (2015) 170–178.
[19] M.S. Liang, R.C. Yang, Y.C. Chiang, D.C. Lyu, R.Y. Lyu, A Taiwanese text-to-speech system with applications to language learning, in: Proc: IEEE International Conference on Advanced Learning Technologies, 2010, pp. 91–95.
[20] S.P. Panda, A.K. Nayak, modified rule-based concatenative technique for intelligible speech synthesis in Indian languages, Adv. Sci. Lett. 22 (2) (2016) 557–563.
[21] A. Manning, N. Amare, A simpler approach to grammar: (re) engineering parts-of-speech instruction to assist efl/esp students, in: Proc: IEEE International Professional Communication Conference, 2007, pp. 1–9.